Two-step controllable electrochemical etching of tungsten scanning probe microscopy tips

Article *in* The Review of scientific instruments · June 2012

DOI: 10.1063/1.4730045 · Source: PubMed

5 authors, including:

Yasser Khan
University of California, Berkeley
23 PUBLICATIONS **498** CITATIONS
SEE PROFILE

Yaping Zhang
12 PUBLICATIONS **176** CITATIONS
SEE PROFILE

Tien Khee Ng
King Abdullah University of Science and Technology
233 PUBLICATIONS **1,504** CITATIONS
SEE PROFILE

AIP | Review of Scientific Instruments

Two-step controllable electrochemical etching of tungsten scanning probe microscopy tips

Yasser Khan, Hisham Al-Falih, Yaping Zhang, Tien Khee Ng, and Boon S. Ooi

Citation: Rev. Sci. Instrum. **83**, 063708 (2012); doi: 10.1063/1.4730045
View online: http://dx.doi.org/10.1063/1.4730045
View Table of Contents: http://rsi.aip.org/resource/1/RSINAK/v83/i6
Published by the American Institute of Physics.

Two-step controllable electrochemical etching of tungsten scanning probe microscopy tips

Yasser Khan, Hisham Al-Falih, Yaping Zhang, Tien Khee Ng, and Boon S. Ooi[a)]
Photonics Laboratory, King Abdullah University of Science and Technology (KAUST), Thuwal 23955-6900, Saudi Arabia

(Received 25 April 2012; accepted 3 June 2012; published online 22 June 2012)

Dynamic electrochemical etching technique is optimized to produce tungsten tips with controllable shape and radius of curvature of less than 10 nm. Nascent features such as "dynamic electrochemical etching" and reverse biasing after "drop-off" are utilized, and "two-step dynamic electrochemical etching" is introduced to produce extremely sharp tips with controllable aspect ratio. Electronic current shut-off time for conventional dc "drop-off" technique is reduced to ∼36 ns using high speed analog electronics. Undesirable variability in tip shape, which is innate to static dc electrochemical etching, is mitigated with novel "dynamic electrochemical etching." Overall, we present a facile and robust approach, whereby using a novel etchant level adjustment mechanism, 30° variability in cone angle and 1.5 mm controllability in cone length were achieved, while routinely producing ultra-sharp probes. © *2012 American Institute of Physics*. [http://dx.doi.org/10.1063/1.4730045]

I. INTRODUCTION

In scanning probe microscopy, sharper tips offer higher performance. Consistency in tip shape and reproducibility are extremely important for both commercial applications and research. Ultra-sharp metal tips are widely used for applications in fields as diverse as nanolithography, nanoelectronics, electrochemistry, cell biology, and electron microscopy. A tremendous amount of work has been done to stabilize tip fabrication technology, since tips have been proven to be indispensable to various scanning probe microscopy techniques. A new era of tip fabrication ushered in after the introduction of scanning tunnelling microscopy (STM) developed by Binnig *et al.* in 1982 (Ref. 1), and atomic force microscopy developed by Binnig, Quate, and Gerber in 1986 (Ref. 2). Sharpness and stiffness of tips determine performances of scanning probe microscopes (SPM).[3–6] Since probe size, shape, and chemical composition at the tip apex decisively influence resolution, the need for controllable and reproducible tips is dire.

A myriad of works has been explored and reported in literature over the years on fabrication of SPM probes. Among various methods explored, electrochemical etching[7–22] proved to be an inexpensive, efficient, and reliable way to fabricate extremely sharp tips. Other reported techniques include cutting,[23,24] grinding,[1–6,25] pulling,[19,26–30] beam deposition,[31–34] ion milling,[35–39] and others. For electrochemical etching, recent advances in tip fabrication came in the form of reverse biasing after "drop-off,"[21] in 2002 and "dynamic electrochemical etching"[40] in 2007. Guise *et al.* optimized etching conditions to produce probes with 5 nm radius of curvature reproducibly.[21] However, tip shapes remained uncontrollable. Hobara *et al.* used dynamic etching technique, where the probe was slowly lifted off from the liquid using a stepper motor, which is a widely adopted method for producing scanning near-field optical microscopy tips. Ju *et al.* employed a similar approach for producing sharp tips, however tips were very long and spindly.[41]

Therefore, we introduce a facile and robust approach that incorporates synergy of "drop-off" method, dynamic electrochemical etching, reverse biasing after "drop-off,"and two-step etching yielding sharp and highly reproducible tips with controllable cone angles. Two-step electrochemical etching routinely produces tips with lower aspect ratio than one-step electrochemical etching. In SPM, tips with high aspect ratio are susceptible to noise as longer probes can pick up signal from side surfaces. Moreover, these spindly tips get damaged easily while handing or in the coarse surface-approach phase in SPM. With two-step controllable electrochemical etching, it is possible to drastically reduce the aspect ratio of tips. Using dynamic etching, a high degree of control can be achieved in cone angle and cone length. Using a simple etchant level mechanism system, we were able to achieve 30° variability in cone angle and 1.5 mm controllability in cone length. While one-step etching routinely produced tips with the radius of curvature (RoC) less than 40 nm with ∼80% success rate, with two-step etching the success rate was enhanced to ∼90% producing tips with RoC less than 10 nm. Reproducibility of the probes was confirmed by optical and scanning electron microscopy analysis.

II. DYNAMIC ELECTROCHEMICAL ETCHING

Electrochemical etching is widely accepted as a fast and reliable method of producing ultra-sharp tips. Additionally, "drop-off" method is a robust technique that provides flexibility in terms of control in etching parameters and process, which is crucial for manufacturing probes with similar shapes. In the "drop-off" technique, a metallic wire is etched using a liquid etchant. The standard way is to dip a wire into an electrolyte, and bias the tip so that etching starts at the air/electrolyte reaction interface and into the immersed

a)Electronic mail: boon.ooi@kaust.edu.sa.

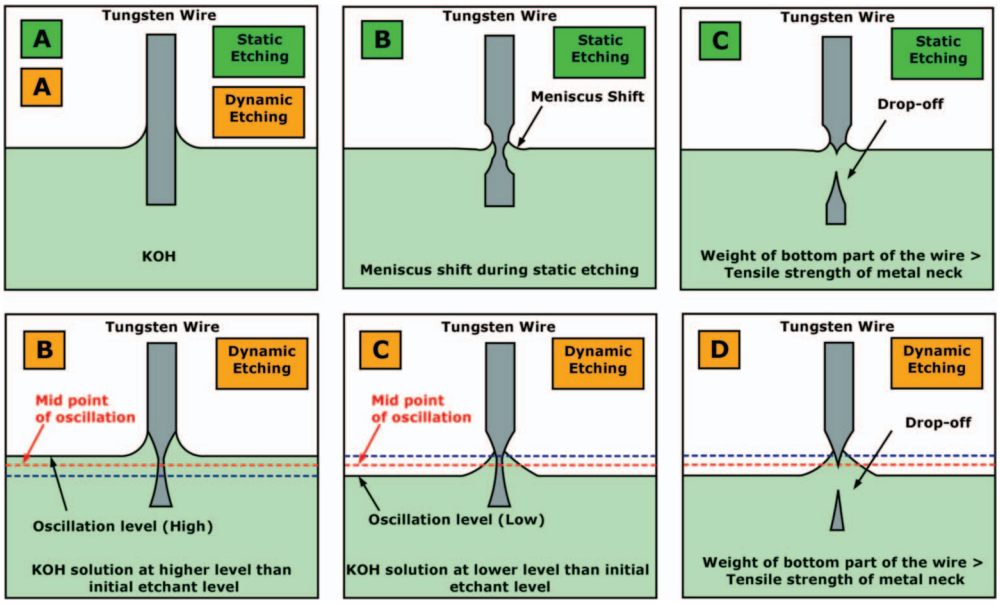

FIG. 1. Juxtapose between static (green A-C) and dynamic (orange A-D) etching. (A) Initial stage for both static and dynamic etching. For static etching (green B), meniscus shifts to lower levels that causes a step-like etching. In (green C), the bottom part of the wire drops off when weight of the bottom piece of the wire becomes higher than the tensile strength of the metallic neck. This "drop-off" abruptly changes etching current, which is used to trigger an external cut-off circuit to stop etching. In the case of dynamic etching (orange B and C), the electrolyte level moves up and down while etching, and prevents meniscus shift and step-like etching. Lastly in (orange D), drop-off occurs in similar fashion to static etching while producing a uniform cone-shaped tip.

metallic wire (depicted in Fig. 1(B)). Choice of electrolytes and dc bias levels depends on the tip material. Usually potassium hydroxide (KOH) is used for tungsten wires. $CaCl_2$, NaCl, or KCl is used for Platinum-Iridium wires.[11] A meniscus is formed at the wire/electrolyte interface. The shape of meniscus determines final tip shape. A complex electrochemical reaction happens at the interface, which is elaborately discussed by Ibe *et al.*,[12] and shown in Eq. (1). On the anode side, tungsten goes through an oxidative dissolution to tungsten anions WO_4^{2-}, which is soluble in water. Additionally, on the cathode side, hydrogen bubbles $H_{2(g)}$ and OH^- are produced:

$$\begin{aligned} \text{cathode} &: 6H_2O + 6e^- \rightarrow 3H_{2(g)} + 6OH^- \\ \text{anode} &: W_{(s)} + 8OH^- \rightarrow WO_4^{2-} + 4H_2O + 6e^- \\ \text{overall} &: W_{(s)} + 2OH^- + 2H_2O \rightarrow WO_4^{2-} + 3H_{2(g)}. \end{aligned} \quad (1)$$

Etch rate follows an incremental gradient from the top to bottom of the meniscus, which is why conical shaped tip apogee is formed. As depicted in the (Fig. 1 (green B)) necking occurs below the air/electrolyte interface, and when the weight of the lower end of the wire becomes greater than the tensile strength of the wire, the bottom piece drops off. A cut-off circuit detects the drop off and shuts down the etching current in ~36 ns. Details on circuit design and etcher setup are discussed in Sec. V.

Shape of tip apex depends on the meniscus that is formed by capillary forces. In the case of static etching, the meniscus shifts over time and the final probe becomes irregular in shape (Fig. 1 (green C)). However, with dynamic etching, the etchant level is changed with a control mechanism (shown in Fig. 1 (orange B and C)). As a result, meniscus shift does not occur, and this technique produces a smooth and uniformly controlled probe shape.

Dc bias level strictly determines etch rate, therefore, wires with small diameters require reduced bias level than wires with wider diameter, otherwise the etch process becomes uncontrollable. Tungsten is the most popular material for STM tips, because tungsten tips can be produced with an electrochemical etch using trivial etchant such as KOH or NaOH. In our study, we used both NaOH and KOH, however, we did not find substantial anomalies in result. We used 10 V dc bias and 1 M KOH on 250 μm diameter wire, and 3 V bias and 1 M KOH on 50 μm diameter wire. KOH pellets and 99.95% tungsten wires were acquired from Sigma Aldrich.

III. CONTROLLING TIP SHAPE AND CONE ANGLE

A problem with static dc etching is undesirable variability tip shapes (Figs. 2(a) and 2(b)). Because the electrolyte solution level remains stagnant throughout the process, the meniscus often moves to a lower level as depicted in (Fig. 1 (green B)). This results in multi-stage etching. Meniscus shift does not follow any specific pattern, which is why probes produced with this technique depict huge anomaly (Figs. 2(a) and 2(b)). In Fig. 2(a), a tip suffered from multi-stage etching by meniscus shift is shown. In Fig. 2(b), an unusable tip that almost got bifurcated in the middle is shown.

A solution to this problem can be achieved through "dynamic etching," where the electrolyte level is vertically raised and lowered, resulting in a smooth and controllable tip shape. This way, meniscus changes with a predefined frequency and yields smooth tips. Two parameters are available to adjust for producing satisfactory results: (i) oscillation amplitude,

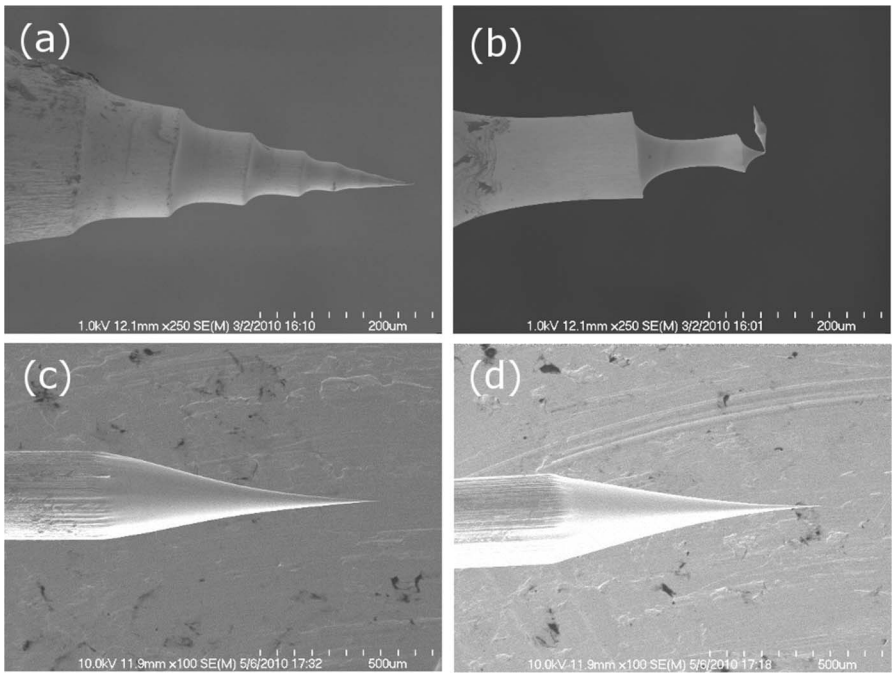

FIG. 2. Scanning electron micrographs of etched tips. (a) and (b) Two probes etched using traditional "drop-off" mechanism in static electrochemical etching. (c) and (d) Two probes etched using "dynamic etching" process. Probe in (a) shows multi-stage etching, which is caused by meniscus shift during various stages of the etching process. Probe in (b) shows a damaged tip, which was nearly bifurcated during the etching process, and thus shows unreliability of the static etching process. Tips in (c) and (d) show smooth and uniform etching with similar shape. Both the tips were etched with 200 μm/s vertical oscillation speed and 1800 μm oscillation amplitude.

which is the vertical height change in the etchant level, and (ii) oscillation frequency, which is the speed of electrolyte level change. Oscillation amplitude determines cone length and cone angle. With optimization, it is possible to change aspect ratio of the probes. With higher oscillation amplitude, cone length (Fig. 3 (`green` curve)) increases, and inversely cone angle (Fig. 3 (`blue` curve)) decreases. Reducing oscillation amplitude decreases cone length and increases cone angle. Oscillation amplitude is determined by the resolution of the etchant level adjustment mechanism. With a simple setup using servo motors, it is possible to change the amplitude from 400 μm to a 3 mm.

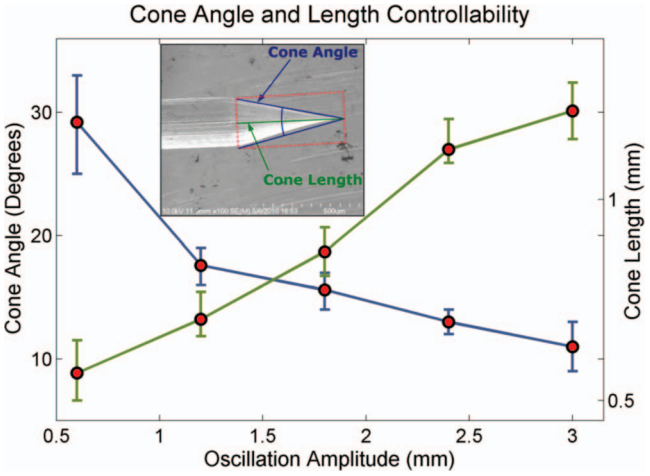

FIG. 3. Tip cone control. For different fluid oscillation amplitudes, cone angles (`blue`) and cone lengths (`green`) are plotted. Each measurement represents at-least five sample points. Cone angle (`blue`) and cone length (`green`) can be controlled by changing oscillation amplitude. Cone length increases almost linearly with oscillation amplitude, while cone angle decreases with increment in oscillation amplitude.

IV. TWO-STEP DYNAMIC ETCHING

While one-step dynamic etching produces sharp tips with controllable cone angles, wire diameter at initial immersion to liquid etchant adds a physical constraint on getting low aspect ratio tips. Meniscus formed at the initial dipping determines the final shape. As a result of that, wires with wider diameters tend to yield a higher aspect ratios than wires with thinner diameters. However, it is inherently difficult to handle thin probes, because they are highly susceptible to mechanical damage. To address this issue, two-step electrochemical etching was introduced. In the first step, the wire is etched for a predefined period of time to reduce thickness and etch out irregular surfaces of a typical tungsten wire. Then the etched wire is re-inserted into the solution, but at a lower immersion depth. After "drop-off" occurs, a sharp tip with aspect ratio lower than one-step etching is produced.

As depicted in Fig. 4, two-step dynamic etching proceeds similar steps as in one-step dynamic etching (Fig. 4 (`orange A-C`)), the wire is dipped 1 mm to 4 mm into the etchant and etched for 10−20 min. After the initial etching, the wire is cleaned with deionized water and isopropyl alcohol, then dried with compressed nitrogen gas. Next, the wire is inspected under an optical microscope for etch profile, and then put re-inserted into the etchant. Second dipping is done in a way so that the meniscus forms between the thinner part of the wire and the electrolyte interface (Fig. 4 (`blue D and E`)).

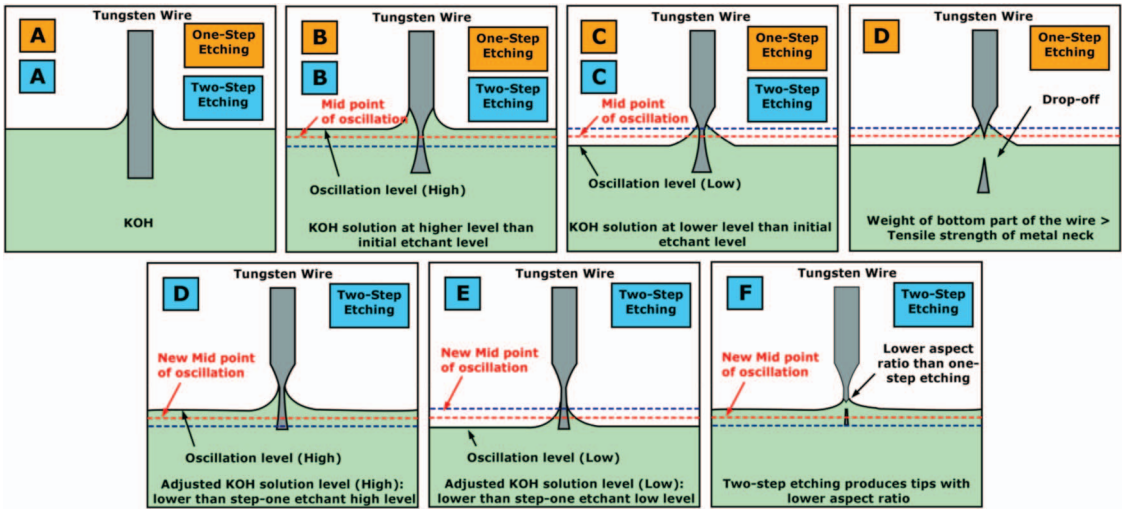

FIG. 4. One-step (orange) and two-step (blue) dynamic electrochemical etching. One-step etching (orange A-D) is essentially previously described dynamic electrochemical etching, where electrolyte level oscillates during the etching process. For two-step etching (blue A-F), the probe is removed from the etchant after a predetermined time of initial etching, and then cleaned and dried. Next, the tip is re-inserted for etching, but at a smaller immersion depth than the first step (blue D and E). Figure (blue F) shows drop-off occurring at a lower height producing a tip with lower aspect ratio than one-step etching.

Depending on the first etching step, the second step completes within 4−12 min. Then, the cut-off circuit triggers and stops etching after the bottom part of the tip is dropped of—producing a probe with a low aspect ratio. Fig. 5 shows a probe after initial etching. Vertical etch rate varies for different types of wire, polycrystalline W, re-crystallized W(110), and single crystal W(111) wires have different vertical etch rate. After determining the vertical etch rate for a specific type of wire, the first step of etching is done for 10−20 min to make a thinner wire. This polycrystalline tungsten wire was reduced to 180 μm from initial diameter of 250 μm in 15 min. Also the necking region shows conical shape, which determines tip shape for one-step etching. For two-step etching, the tip is inserted into the etchant at a lower level engendering a new meniscus that later translates to a sharp tip with lower aspect ratio.

Ju *et al.* recently reported controllability in terms of aspect ratio, where dynamic etching was used to slowly lift off tungsten wires from electrolyte.[41] Although this technique offers control over aspect ratio, produced tips were long and spindly because lifting of from etchant provides freedom only on the positive z-axis. With two-step dynamic etching, it is possible to create extremely sharp tips, and at the same time, reduce aspect ratio. Additionally, in our previous work, we saw two-step etching provides better results than one-step etching in term of radius of curvature.[42] Some applications, such as STM, require extremely sharp tips of low aspect ratio, two-step etching provides that control in both aspect ratio and RoC. In Fig. 6(a), a two-step electrochemically etched tip is shown. Approximating from the etch profile the orange rectangle of length 822 μm and width 232 μm: aspect ratio of 3.54, provides estimated tip shape. The blue rectangle of 214 μm and width 60 μm: aspect ratio of 3.56, is the tip shape yielding from the second-step of two-step etching. Almost equal aspect ratio in both the cases implies similar etching in first and second step of etching. As a result of two-step etching, overall length becomes 647 μm, and taking the initial width of 232 μm, aspect ratio reduces to 2.78. Reduction in the aspect ratio is vital for scanning electron microscopy. Since existing techniques yield tips with high aspect ratio, for STM applications, slightly blunt tips with low aspect ratio are used. Then these tips are sharpened further with field directed sputter sharpening.[43] Using an optimized two-step dynamic electrochemical etching method, tip production for STM can be simplified by manufacturing extremely sharp tips with low aspect ratio only with electrochemical etching. In Fig. 6(b), uniform etching at tip apex is shown, producing the radius of curvature less than 10 nm.

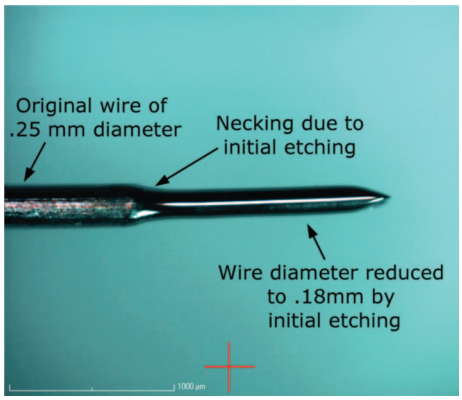

FIG. 5. Optical micrograph of a wire after initial etching of 15 min. Wire diameter is reduced from 250 μm to 180 μm, and the necking region, which occurs due to etching in air/electrolyte interface is also apparent.

V. ELECTRONIC CIRCUIT DESIGN AND ETCHER SETUP

Conventional electrochemical etching usually utilizes a control circuit for sensing "drop-off" to trigger a signal that abruptly stops etching current. To attain further control such as dynamic etching and reverse bias after "drop-off," additional circuitry is required. To reduce complexity, circuitry

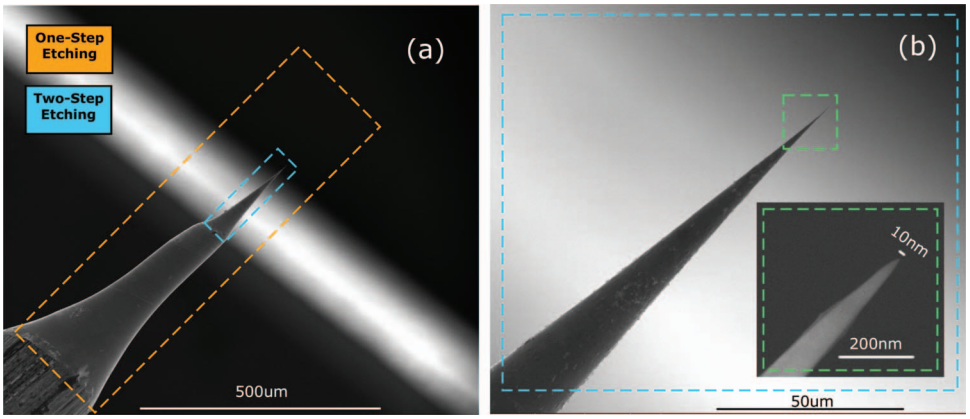

FIG. 6. Scanning electron micrographs of a tip etched by two-step electrochemical etching. In (a), estimated shape of one-step etching (`orange`) rectangle and the actual shape for two-step etching (`blue`) rectangle is shown. For one-step etching, predicted shape (`orange`) rectangle has length 822 μm and width 232 μm, therefore giving an aspect ratio of 3.54. In the case of two-step etching, the (`blue`) rectangle has length 214 μm and width 60 μm, therefore giving an aspect ratio of 3.56. Because of two-step etching, overall length becomes 647 μm, and provides an aspect ratio of 2.78. (b) Uniform etching at tip apex, and the inset (SEM with high magnification—`green` rectangle) shows radius of curvature less than 10 nm.

was modularized, and "drop-off" sensing circuit and dynamic control circuit were kept aloof. This modular setup proved vital for "drop-off" circuit to trigger, because external electrical perturbation affects the performance of the high speed trigger circuit.

Basic control for the system was provided by a Arduino micro-controller. Arduinos are low-cost and popular micro-controllers, and have extensive programming resources. For executing computer codes and real-time system monitoring, these micro-controllers are quite handy. A daughter-card was designed for housing control circuit and cut-off circuit. Etchant level control was provided through servo motors interfaced with Arduino. Lastly, an etch cell, which hosted the tungsten tip, counter electrode (stainless steel/tungsten) and mechanism for changing KOH level inside the etch cell were placed on a vibration isolation table to reduce external disturbance. It has been observed that vibration from counter electrode or external sources creates abysmal effect on tip shape. Therefore, the etch cell was designed to isolate bubbling of $H_{2(g)}$ on the cathode side from the anode side of the cell.

Universal serial bus interface gives direct access to the Arduino board (Fig. 7). Using a computer, system code can be uploaded to the Arduino board. Arduino mainly controls the etchant level adjustment mechanism, detects etchant levels during etching, and senses drop off signal. When the system is powered up, solution level starts to rise, and when the tip touches the solution, Arduino receives a logic high. Then, solution level rises to a pre-determined height of 1 mm to 4 mm, and starts oscillating. If the bottom part of the tip drops off another logic high signal is generated and sent to both cut-off circuit and the Arduino. Cut-off circuit shuts down voltage very quickly (~36 ns), and Arduino lowers solution level so that the tip does not remain in contact of KOH. ~36 ns cut-off time is a significant improvement over currently reported etching current cut-off time, Jobbins, Raigoza, and Kandel reported cut-off time in the range of 0.5−1 μs. (Ref. 44). Moreover, most "drop-off" detection system are based on digital signal processing (DSP), in our system, we employ high-speed analog electronics to sense "drop-off." This makes external DSP based control redundant.

Guise *et al.* reported that natural potential difference between counter electrode and the W tip causes tip blunting even after fast current shut off, and reverse biasing after "drop-off" takes care of the mentioned issue.[21] We employed a similar technique of reverse biasing. Differences in tip RoC for reverse biasing and grounding after drop-off were apparent. Reverse bias sets the tip voltage at −1 V after "drop-off,"

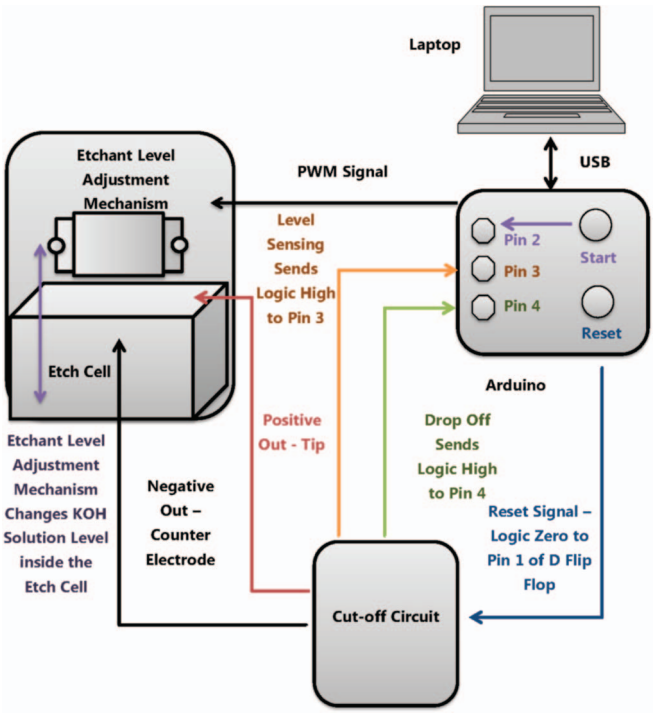

FIG. 7. System block diagram. Complete system setup is modularized into four segments: (i) `Laptop` provides computer control to the etching process and simultaneously monitors real-time etching current and etchant level. (ii) `Arduino` interfaced with a daughter card maintains the etchant level control mechanism and, at the same time, senses etchant level. (iii) `Cut-off Circuit Board` houses high speed differentiator for generating drop-off signal, when the bottom part of the tip drops off. (iv) `Etch cell` is placed on a vibration isolation table to reduce external perturbation. This cell holds the tip, which is (`positive`) biased, and the counter electrode that is (`negative`) biased.

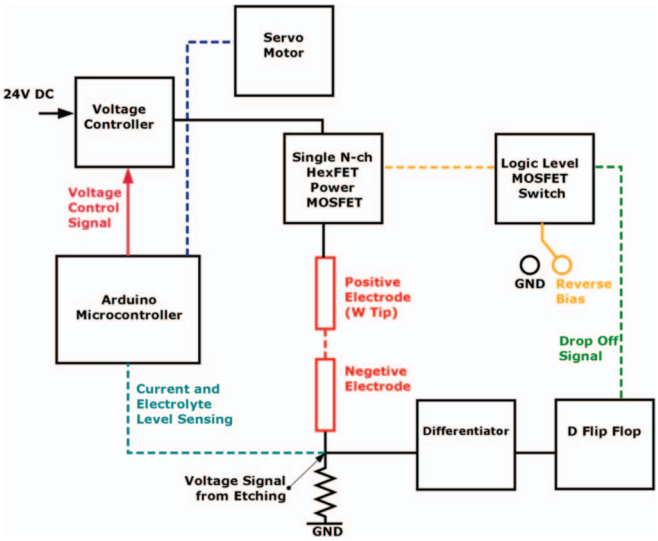

FIG. 8. Circuit design for etcher. Control circuit is essentially the well reported "drop-off" sensing circuit with advanced electronics and additional features for providing dynamic etching via the `servo motor` connection, and reverse-biasing after drop off (`yellow` solid line). An external power source provides 24 V dc voltage that can be controlled by Arduino. This is fed to a single N-channel HexFET Power MOSFET, and used for etching probes (`red` positive electrode). Signal from the counter electrode is converted to a voltage signal using a 500 Ω resistor. This voltage signal provides both etching current signal (to the differentiator circuit) and electrolyte level signal (`blue` dotted line to Arduino). When the bottom part of the wire breaks, a logic high is generated and sent to a MOSFET switch (`green` dotted line) to stop etch process.

thus stops etching altogether, producing ultra-fine tips. We designed circuitry to operate in both reverse bias (−1 V) and ground (0 V) options. At the time of drop-off, the cut-off circuit senses voltage signal (Fig. 8. (circuit block diagram)) that signal is passed through a high speed differentiator. This differentiator inverts the signal, (Fig. 9) $V_{out} = -RC\frac{dV_{in}}{dt}$, and then uses the positive edge to trigger a D Flip-Flop, which stops etching current.

For polycrystalline tungsten wires of 250 μm diameter, $R = 3.5$ KΩ, and $C = 0.01\,\mu$F is used in the differentiator

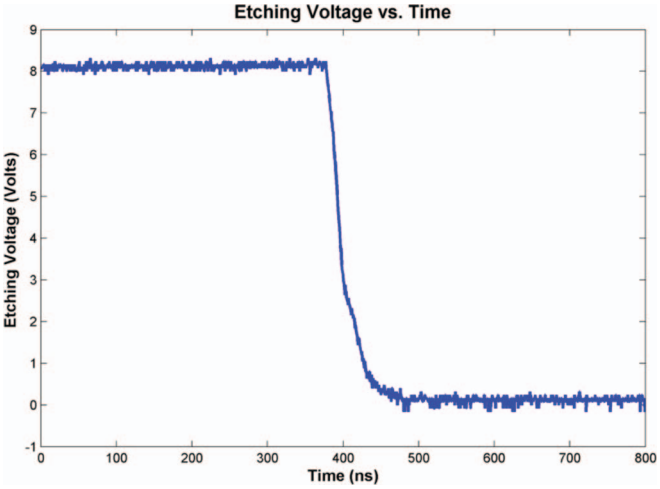

FIG. 9. Etching voltage snapshot during "drop-off." A high speed differentiator cuts off etching voltage in less than 40 ns. This can also be reconfigured to provide reverse bias at the tip-end after "drop-off" occurs.

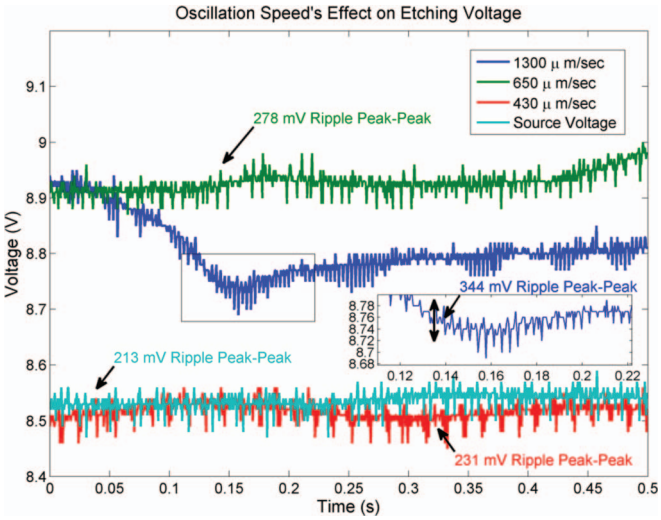

FIG. 10. Dynamic etching voltage depends on etchant oscillation speed. For high speed such as 1300 μm/s (`blue` curve), there are significant ripples in etching voltage (344 mV peak–peak). With reduced speed of 650 μm/s (`green` curve) and 430 μm/s (`red` curve) the ripples are reduced to 278 mV peak–peak and 231 mV peak–peak, while source voltage ripple (`cyan` curve) is around 213 mV peak–peak.

circuit. Depending on the tip material and different wire diameter, these R and C need to be optimized, because drop-off signal varies with different wire types. The signal out from the differentiator at the time of drop-off is used to trigger a positive edge triggered D Flip-Flop (Fig. 8). Then the drop-off signal through a logic level MOSFET shuts down voltage supply and reverse biases the tip to −1 V or ground, depending on the initial circuit setup. Since the Arduino lowers the solution level at almost the same time, concern of re-depositing material on the tip is avoided. After drop-off occurs, it is essential to clean the tip instantly with deionized water, and then with acetone and ethanol. This step cleans up residues left after etching. Then, tip is dried with compressed nitrogen gas.

While oscillation amplitude determines tip cone angle and cone length, oscillation frequency has direct effect on etching voltage, higher speed such as 1300 μm/s creates unwanted disturbance in etching voltage (Fig. 10 (`blue` curve)), also creates etchant liquid turbulence inside the cell. This perturbation creates issues in cut-off circuitry in the form of false triggering. Lower speed leads to more stable etching voltage (Fig. 10 (`red` curve)), however too slow speed leads to multi-state etching. The value of 325 μm/s proved to give a stable etching voltage, while preventing multi-state etching. Additionally, higher oscillation speed may cause curling at tip end after drop-off. The weight of the drop-off piece and vertical oscillation speed are factors effecting tip shape at the apex. Heavy drop-off piece may exert high force while falling off from the top part, as a result the probe gets curled at the apex, creating an unusable probe for microscopy.

VI. CONCLUSIONS

There is a vast amount of reported techniques to make SPM tips, and these techniques do yield really sharp tips. But, reproducibility and controlling tip shape becomes an issue.

Recent efforts in stabilizing tip fabrication came in the form of reverse biasing after "drop-off,"[21] and "dynamic electrochemical etching."[40] However, tips remained very long and spindly.[41] Extremely sharp tips with low aspect ratio are vital for scanning tunnelling microscopy, and eventually atomically precise manufacturing.[45] We tried to address these issues by using well-established procedures from literature, and facilitating that with "dynamic etching" and computer control. Synergy of "drop-off" method, "dynamic electrochemical etching," and reverse biasing after "drop-off" produced highly reproducible tips with controllable cone angles. Using a novel etchant level adjustment mechanism, 30° variability in cone angle and 1.5 mm controllability in cone length was achieved. While one-step etching routinely produced tips with RoC less than 40 nm with ~80% success rate, with the novel two-step etching, the success rate was enhanced to ~90%, producing tips with RoC less than 10 nm.

We explored numerous parameters effecting the etching process. Etching voltage was optimized so that it was high enough to create drop-off, but not very high to produce blobbing at tip apex. High KOH concentration was found to create turbulent bubbles on the cathode side, therefore, KOH concentration was kept to an adequate level where reaction rate was not violent. Cathode was put in an isolated compartment to create fluid vibration isolation. Since meniscus shape directly affects tip apex, we tried to fix the tip at 90° to the etchant, and changed KOH level for "dynamic-etching" while keeping the tip fixed. With two-step electrochemical etching, we were able to produce low aspect ratio tips from 250 μm diameter tungsten wires. Oscillation amplitude for dynamic etching determined final tip shape. In addition, oscillation frequency directly effected etching voltage, and higher speed translated into significantly high ripples in etching voltage, 325 μm/s proved to give a stable etching voltage, while preventing multi-state etching. Overall, in this work, we performed a complete study to produce tips reproducibly with control on tip shape, and optimized etching conditions reported in literature, and added new features of "two-step dynamic electrochemical etching" and computer control. With two-step dynamic etching, smooth low aspect ratio probes with RoC less than 10 nm were routinely produced.

ACKNOWLEDGMENTS

The authors are grateful for the generous funding from the KAUST. Hisham Al-Falih would like to thank the Saudi Research Science Institute for their summer internship support. Initial phase of the work was done at the Zyvex Labs, supported by funding from the Defense Advanced Research Projects Agency (DARPA) (Contract No. N66001-08-C-2040), and a grant from the Emerging Technology Fund of the State of Texas. Yasser Khan would like to acknowledge valuable suggestions and guidance from Josh Ballard, Justin Alexander, John Randall, and Jim Von Ehr from the Zyvex Labs.

[1]G. Binnig, H. Rohrer, C. Gerber, and E. Weibel, Phys. Rev. Lett. **49**, 57 (1982).
[2]G. Binnig, C. F. Quate, and C. Gerber, Phys. Rev. Lett. **56**, 930 (1986).
[3]H. Y. Liu, F. R. F. Fan, C. W. Lin, and A. J. Bard, J. Am. Chem. Soc. **108**, 3838 (1986).
[4]C. M. Mate, G. M. McClelland, R. Erlandsson, and S. Chiang, Phys. Rev. Lett. **59**, 1942 (1987).
[5]R. Wiesendanger, H.-J. Güntherodt, G. Güntherodt, R. J. Gambino, and R. Ruf, Phys. Rev. Lett. **65**, 247 (1990).
[6]M. Nonnenmacher, M. P. O'Boyle, and H. K. Wickramasinghe, Appl. Phys. Lett. **58**, 2921 (1991).
[7]P. J. Bryant, H. S. Kim, Y. C. Zheng, and R. Yang, Rev. Sci. Instrum. **58**, 1115 (1987).
[8]A. Cricenti, S. Selci, R. Generosi, E. Gori, and G. Chiarotti, Solid State Commun. **70**, 897 (1989).
[9]M. Yata, M. Ozaki, S. Sakata, T. Yamada, A. Kohno, and M. Aono, Jpn. J. Appl. Phys. **28**, L885 (1989).
[10]L. Libioulle, Y. Houbion, and J.-M. Gilles, J. Vac. Sci. Technol. B **13**, 1325 (1995).
[11]A. J. Nam, A. Teren, T. A. Lusby, and A. J. Melmed, J. Vac. Sci. Technol. B **13**, 1556 (1995).
[12]J. P. Ibe, J. P. P. Bey, S. L. Brandow, R. A. Brizzolara, N. A. Burnham, D. P. DiLella, K. P. Lee, C. R. K. Marrian, and R. J. Colton, J. Vac. Sci. Technol. A **8**, 3570 (1990).
[13]J. P. Song, N. H. Pryds, K. Glejbol, K. A. Morch, A. R. Tholen, and L. N. Christensen, Rev. Sci. Instrum. **64**, 900 (1993).
[14]H. Lemke, T. Goddenhenrich, H. P. Bochem, U. Hartmann, and C. Heiden, Rev. Sci. Instrum. **61**, 2538 (1990).
[15]A. I. Oliva, A. Romero G., J. L. Peña, E. Anguiano, and M. Aguilar, Rev. Sci. Instrum. **67**, 1917 (1996).
[16]Y.-G. Kim, E.-H. Choi, S.-O. Kang, and G. Cho, J. Vac. Sci. Technol. B **16**, 2079 (1998).
[17]L. A. Hockett and S. E. Creager, Rev. Sci. Instrum. **64**, 263 (1993).
[18]H. Muramatsu, K. Homma, N. Chiba, N. Yamamoto, and A. Egawa, J. Microsc. **194**, 383 (1999).
[19]A. Lazarev, N. Fang, Q. Luo, and X. Zhang, Rev. Sci. Instrum. **74**, 3684 (2003).
[20]S. Patan, E. Cefal, A. Arena, P. Gucciardi, and M. Allegrini, Ultramicroscopy **106**, 475 (2006).
[21]O. L. Guise, J. W. Ahner, M.-C. Jung, P. C. Goughnour, and J. T. Yates, Nano Lett. **2**, 191 (2002), http://pubs.acs.org/doi/pdf/10.1021/nl010094q.
[22]O. Naaman, W. Teizer, and R. C. Dynes, Rev. Sci. Instrum. **72**, 1688 (2001).
[23]J. Garnaes, F. Kragh, K. A. Morch, and A. R. Tholen, J. Vac. Sci. Technol. A **8**, 441 (1990).
[24]A. A. Gorbunov, B. Wolf, and J. Edelmann, Rev. Sci. Instrum. **64**, 2393 (1993).
[25]T. Held, S. Emonin, O. Marti, and O. Hollricher, Rev. Sci. Instrum. **71**, 3118 (2000).
[26]E. Betzig, J. K. Trautman, T. D. Harris, J. S. Weiner, and R. L. Kostelak, Science **251**, 1468 (1991).
[27]B. I. Yakobson, P. J. Moyer, and M. A. Paesler, J. Appl. Phys. **73**, 7984 (1993).
[28]G. A. Valaskovic, M. Holton, and G. H. Morrison, Appl. Opt. **34**, 1215 (1995).
[29]M. Xiao, J. Nieto, R. Machorro, J. Siqueiros, and H. Escamilla, J. Vac. Sci. Technol. B **15**, 1516 (1997).
[30]N. Essaidi, Y. Chen, V. Kottler, E. Cambril, C. Mayeux, N. Ronarch, and C. Vieu, Appl. Opt. **37**, 609 (1998).
[31]Y. Akama, E. Nishimura, A. Sakai, and H. Murakami, J. Vac. Sci. Technol. A **8**, 429 (1990).
[32]K. L. Lee, D. W. Abraham, F. Secord, and L. Landstein, J. Vac. Sci. Technol. B **9**, 3562 (1991).
[33]B. Hbner, H. Koops, H. Pagnia, N. Sotnik, J. Urban, and M. Weber, Ultramicroscopy **4244** (Part 2), 1519 (1992).
[34]M. Wendel, H. Lorenz, and J. P. Kotthaus, Appl. Phys. Lett. **67**, 3732 (1995).
[35]D. K. Biegelsen, F. A. Ponce, J. C. Tramontana, and S. M. Koch, Appl. Phys. Lett. **50**, 696 (1987).
[36]D. K. Biegelsen, F. A. Ponce, and J. C. Tramontana, Appl. Phys. Lett. **54**, 1223 (1989).
[37]H. Ximen and P. E. Russell, Ultramicroscopy **4244** (Part 2), 1526 (1992).
[38]P. Hoffrogge, H. Kopf, and R. Reichelt, J. Appl. Phys. **90**, 5322 (2001).
[39]K. Akiyama, T. Eguchi, T. An, Y. Fujikawa, Y. Yamada-Takamura, T. Sakurai, and Y. Hasegawa, Rev. Sci. Instrum. **76**, 033705 (2005).
[40]R. Hobara, S. Yoshimoto, S. Hasegawa, and K. Sakamoto, J. Surf. Sci. Nanotechnol. **5**, 94 (2007).
[41]B.-F. Ju, Y.-L. Chen, and Y. Ge, Rev. Sci. Instrum. **82**, 013707 (2011).

[42]H. Al-Falih, Y. Khan, Y. Zhang, D. San-Roman-Alerigi, D. Cha, B. S. Ooi, and T. K. Ng, in *High Capacity Optical Networks and Enabling Technologies (HONET), 2011* (2011), pp. 190–192.
[43]S. W. S. Joseph and W. Lyding, "Nanometer-scale sharpening of conductor tips," U.S. patent 8,070,920 (2011).
[44]M. M. Jobbins, A. F. Raigoza, and S. A. Kandel, Rev. Sci. Instrum. **83**, 036105 (2012).
[45]Y. Khan and J. Randall, in *Proceedings of the Eighth International Conference on Information Technology: New Generations (ITNG)* (2011), pp. 965–969.